Recording beam modulation during grating formation

Michael R. Gleeson, John V. Kelly, Feidhlim T. O'Neill, and John T. Sheridan

Holography has been of increasing interest in recent years, with developments in many areas such as data storage and metrology. Photopolymer materials provide potentially good materials for holographic recording, as they are inexpensive and self-processing. Many experiments have been reported in the literature that describe the diffraction efficiency and angular selectivity of such materials. The majority of these reports discuss the performance of the holographic optical element after the recording stage. It has been observed, however, that sometimes, during exposure, the transmitted recording beam intensities vary with time. A simple phenomenological model is proposed to explain the beam modulation, which incorporates the growth of the phase grating, time-varying absorption effects, the mechanical motion of the plate, the growth of a lossy absorption grating during the recording process, and the effects of nonideal beam ratios.

OCIS codes: 090.0090, 090.2900, 090.2890, 090.2890, 160.5470.

1. Introduction

In recording a sinusoidal unslanted holographic grating in a photopolymer material[1] we have observed,[2,3] as have others,[4] that the intensities of the two transmitted beams occasionally fluctuate in an approximately sinusoidal fashion. Significantly, this variation in the intensities does not always occur. In this paper we provide one possible explanation for such behavior. Analysis of the recording process is carried out, and an approximate model of the behavior is proposed. The resultant predictions are compared with experimental data.

In the proposed model we attempt to take into account four effects, namely, (i) any in-plane motion of the grating with respect to the two exposing beams, (ii) the time-varying absorption of the photopolymer material that is due to bleaching of the photosensitive dye, (iii) the growth of the phase grating owing to the increase in the refractive-index modulation, and, finally, (iv) the existence of a lossy absorption grating during exposure. As the lossless grating is being formed, an absorption grating will be formed simultaneously because of the reduction in dye concentration in the exposed regions of the grating. Therefore a lossy grating is formed exactly out of phase with the refractive-index grating. The effects of this absorption or lossy grating are examined in an attempt to increase the accuracy of the approximate analysis.

We propose that the variations in the transmitted recording intensities during exposure arise primarily as a result of a combination of these effects. We have carried out a series of experiments to examine the validity of our proposed model. The first experiment involves measuring the transmitted intensities of the two exposing beams to examine their variation as a function of time. The second examines the effect that the absorption of the material has on a single beam. The third experiment examines the change in the refractive index that takes place during the growth of the phase grating. The fourth and final experiment carried out involves the estimation of the in-plane mechanical motion of the grating with respect to the two exposing beams.

We present these experiments and, following analysis, show that our model approximately predicts the intensities of the beams during the recording process. Thus our first-order model is shown to be in general agreement with our experimental results.

2. Transmitted Beam Intensity Variations

In this section we briefly outline the first experiment used to monitor the variations of the two recording beams during the recording of a grating and the theoretical notation used.

The authors are with the Department of Electronic and Electrical Engineering, Faculty of Engineering and Architecture, University College Dublin, Belfield, Dublin 4, Republic of Ireland. J. T. Sheridan's e-mail address is john.sheridan@ucd.ie.

Received 10 September 2004; revised manuscript received 25 April 2005; accepted 27 April 2005.

0003-6935/05/265475-08$15.00/0

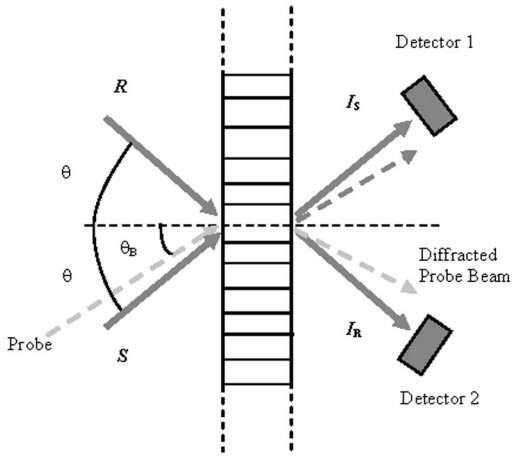

Fig. 1. Schematic of the recording geometry used and the probe beam.

A. Experimental Setup

Shown in Fig. 1 is the experimental setup, which enables both transmitted beams to be observed in real time during recording. The power of both beams was measured before they entered the material. The effect of the material on the two beams was then monitored during and immediately after exposure. The unslanted sinusoidal transmission volume hologram shown in Fig. 1 was recorded by use of a HeNe laser of wavelength $\lambda = 633$ nm. Our photopolymer material consists of a monomer (acrylamide), a binder [poly(vinyl alcohol)], a cross linker (bisacrylamide), a photosensitive dye (Methylene Blue) for recording with the HeNe laser, and an electron donor (triethanolamine).[5] A probe beam of wavelength $\lambda = 488$ nm, which does not interact with the dye, is also used. The transmitted light intensity is measured with an appropriate number of samples per second, and the data are processed with LabView software.[6] One of the experimental data sets obtained is shown in Fig. 2.

We note that a less than ideally stable plate holder was used during this experiment. As can be seen, the intensity of I_R is greater than that of I_S (this is not always the case), which corresponds to exposure with a nonunity or nonideal beam ratio.

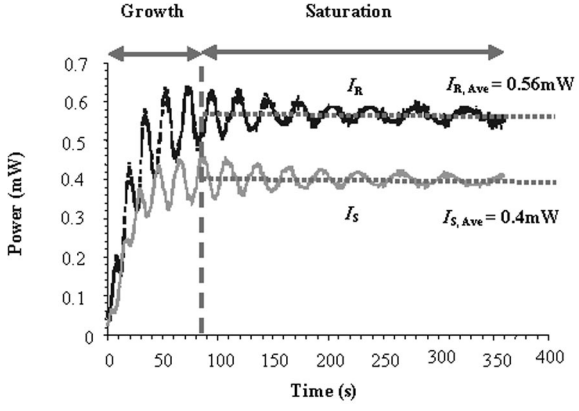

Fig. 2. Transmitted exposing beam intensities. Variation with time of the intensities can be seen for the nonunity beam ratio.

B. Theoretical Notation

Using Kogelnik's notation[7] yields the following expressions for permitivity ε and conductivity σ:

$$\varepsilon = \varepsilon_0 + \varepsilon_1 \cos(Kx), \tag{1}$$

$$\sigma = \sigma_0 - \sigma_1 \cos(Kx), \tag{2}$$

where ε_1 and σ_1 are the amplitudes of the spatial modulations, ε_0 is the average dielectric constant, and σ_0 is the average conductivity. Grating vector magnitude K is given by $2\pi/\Lambda$, where Λ is the period of the grating. In Kogelnik's analysis,[7] ε and σ are assumed to be modulated in phase. In Eq. (2) we introduce a phase shift of π rad, resulting in a change of sign. The expression for coupling constant κ is then

$$\kappa = \frac{1}{4}\left[\frac{2\pi}{\lambda}\frac{\varepsilon_1}{(\varepsilon_0)^{1/2}} + \frac{j\mu c\sigma_1}{(\varepsilon_0)^{1/2}}\right], \tag{3}$$

where λ is the replay wavelength in free space, $\mu = \mu_0$ is the permeability of the medium, which is assumed to be equal to that of free space, and c is the speed of light *in vacuo*. This coupling constant describes the coupling between the two beams that is due to both the phase and lossy gratings, and it can be rewritten as

$$\kappa = \frac{\pi n_1}{\lambda} + \frac{j\alpha_1}{2} = \kappa_r + j\kappa_i, \tag{4}$$

where n_1 is the amplitude of the spatial modulation of the refractive index as in Ref. 7, $\alpha_1 = \mu c\sigma_1/(\varepsilon_0)^{1/2}$ is the amplitude of the absorption modulation associated with the lossy dye grating, and κ_r and κ_i are the real and imaginary parts, respectively, of the coupling constant.

3. Absorption Parameters (α_0, α_1)

The major effects involved in the recording of a grating must be separated (decoupled) to enable a simple phenomenological model of the modulation of the transmitted recording beams to be constructed. The second experiment measured the variation of the absorption of the material with time $\alpha_0(t)$, which was achieved by passage of a single beam through a standard (chemical composition and thickness) material layer. The variation of the resultant transmitted intensity was measured many times, and an average plot was obtained. Time-varying absorption effects caused by the material take place primarily because of the photosensitive dye present in the material. As the light is passed through the material, the dye undergoes an oxidation reaction. The dye absorbs a photon in the presence of the electron donor, which then produces free radicals. These cause the polymerization of the acrylamide, which causes a density vari-

ation in the material and a change in the refractive index.[5] The absorbance of light by the dye is necessary to produce this photochemical reaction. During the early stages of the exposure, more light is absorbed as more active dye is available, but, as the dye is used up (bleached), more and more of the light passes through the material.[8–10] This explains the observed increase in transmitted intensity with time shown in Fig. 3.

To estimate the value of the absorption $\alpha_0(t)$, we processed the data obtained from these experiments. The intensity values measured at the start were nonzero, as the material is partially transparent; the material begins to absorb light as soon as light is incident upon it. A best fit to the data of Fig. 3 was obtained. The resultant analytic fit to the output intensity in terms of parameters $a0$, $a1$, and $a2$ was then substituted into Eq. (5). The result is an empirical expression for the time evolution of absorption $\alpha_0(t)$ as defined for use in Kogelnik's coupled-wave equations (7):

$$\alpha_0(t) = -\frac{\log_e\{1 - \exp[-a0 - a1(t-2) - a2(t-2)^2]\}}{2 \times d}, \tag{5}$$

where d is the measured thickness of the material layer. (The shift in time is included to allow for the inhibition period; see Ref. 11.) The coefficient values obtained are $a0 = 0.235$, $a1 = 0.024$, and $a2 = 0$. A plot of the resultant absorption $\alpha_0(t)$ is shown in Fig. 4.

As was mentioned above, a lossy grating that is π rad out of phase is generated simultaneously as the lossless phase grating is being formed, with $\alpha_1(t)$ the absorption modulation associated with it.[8,12] $\alpha_1(t)$ might reasonably be expected to have a form similar to that shown in Fig. 5, which is governed by an equation of the form

$$\alpha_1(t) = \exp(-pt)[1 - \exp(-qt)]. \tag{6}$$

When the light is incident upon the material the dye absorbs some of the light in the bright regions. As shown in Fig. 5, we propose that $\alpha_1(t)$ initially increase in region t1, as there is an abundance of dye in the bright region and this dye is being bleached by the exposure of the light. Eventually, however, the lossy amplitude reaches a maximum, region t2, and then starts to decrease as the dye available in the bright region is used up and the dye is bleached throughout the volume. The lossy grating amplitude would then be expected to decrease to zero, as shown in region t3. We use this heuristic description of the lossy grating amplitude's temporal behavior in Section 6 below.

Next we examine the effect of the growth of the lossless phase grating on the modulation of the two recording beams.

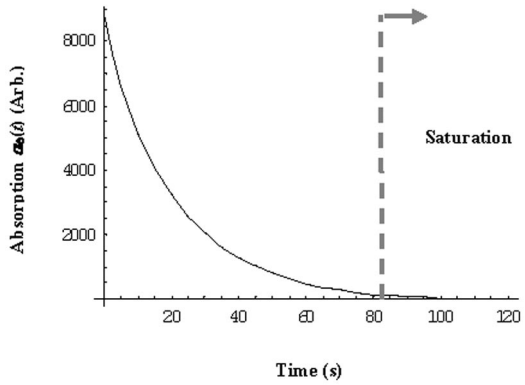

Fig. 4. Change in absorption with time $\alpha_0(t)$.

4. Grating Strength (ν)

As a grating is formed by the creation of a modulation in refractive index n_1, absorption grating $\alpha_1(t)$, or both, coupling takes place between the exposing beams used to record the grating.[13,14] When coupling constant $\kappa = 0$, there is no coupling and therefore there is no diffraction. To enable a value for κ_r to be obtained from the measured experimental data, we captured a growth curve[15,16] by using a probe beam with a wavelength that does not interact greatly with the dye or affect the grating being recorded; see Fig.

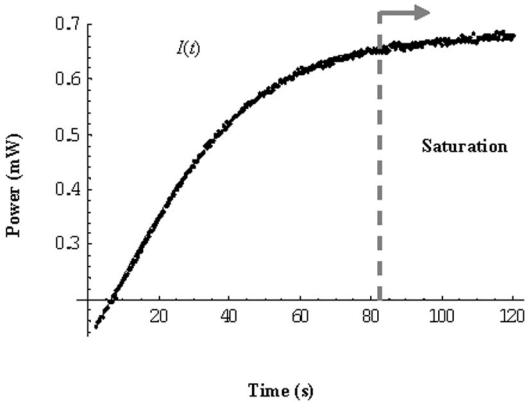

Fig. 3. Single beam (standard layer) fit to the loss data with time.

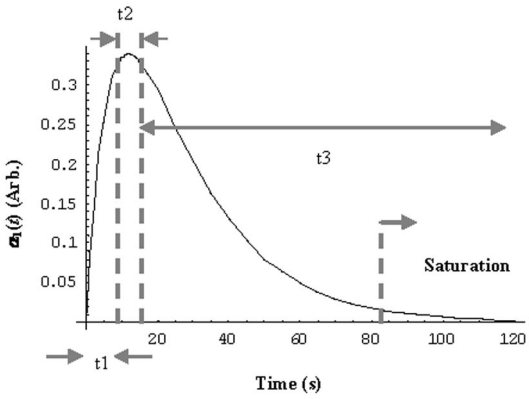

Fig. 5. Example of the form that $\alpha_1(t)$ might be expected to take with time, where $p = 0.05$ and $q = 0.08$.

1. In this case the lossy grating has no effect on the probe beam. The wavelength of the probe beam used is $\lambda = 488$ nm.

In the third experiment we examine the change in the refractive index caused by the growth of the phase grating. Using the growth curve data, we find an expression for the grating strength, ν. To increase the accuracy of our results, we correct the data to allow for Fresnel reflections at the boundaries of the material layer.[17–19] As the refractive index of air is different from that of the photopolymer material and the glass substrate, and while we assume that the refractive index of the material layer is close to that of glass, there are changes in the angles of refraction across the interfaces. Furthermore, reflections from the surfaces reduce the intensity of the transmitted beams. This reduction in intensity will change the measured diffraction efficiencies, and therefore the data must be corrected for these effects. We use Snell's law to calculate the angle at which the light travels within the photopolymer material, $n_r \sin \theta_r = n_i \sin \theta_i$, where n_r is the refractive index of the material that the light is passing into (holographic layer–air), n_i is the refractive index of the material that the light is passing from (air–holographic layer), θ_i is the angle of incidence, and θ_r is the refracted angle inside the material. For the results reported here the refractive index of free space used is $n_i \cong 1$, while the refractive indices of the glass plates and the polymer layer are assumed to be identical, $n_r \cong 1.5$.

The angle of incidence of the exposing beam in air is $\theta_1 = 18.5°$, giving a grating period of $\Lambda = 1$ μm for $\lambda = 633$ nm and $\theta_r = 12.2°$. Applying the Fresnel transmission and reflection coefficients yields the resultant values for the correct diffraction efficiencies. The probe-beam wavelength used was $\lambda = 488$ nm, and the wave was incident on-Bragg in air at $\theta_i = 13.5°$.

The expression derived by Kogelnik[7] for the diffraction efficiency of a lossless phase transmission grating replayed on-Bragg, θ_B, can be used to give an expression for the grating strength:

$$\nu(t) = \sin^{-1}[\sqrt{\eta_{FC}(t)}], \tag{7}$$

where $\eta_{FC}(t)$ is the time-dependent Fresnel-corrected diffraction efficiency. The variation of the grating strength, $\nu(t)$, is then found by application of Eq. (7) to the Fresnel-corrected data. The following function was then used to provide a best fit:

$$\nu(t) = F_0[1 - \exp(-f_1 t + f_2 t^2)]. \tag{8}$$

Typical best-fit coefficient values are $F_0 = 0.606$, $f_1 = 0.247$, and $f_2 = 0.00053$. From Eq. (8), values for the real part of coupling constant $\kappa_r(t)$ can be obtained by use of the following equation:

$$\nu(t) = \frac{\kappa_r(t) d}{\cos \theta_B}. \tag{9}$$

Because the probe beam used has a different wavelength ($\lambda = 488$ nm) we assume that the lossy grating has no effect and that θ_B is the on-Bragg replay angle for that wavelength. In Eq. (9) the thickness of the material has the measured value $d \cong 100$ μm.

When no monomer remains in the layer (when it has all been polymerized), grating formation ends. By this time in the exposure process the refractive index of modulation, n_1, has reached its maximum (saturation) value and it, κ, and ν all remain constant. In Fig. 2, saturation occurs at an exposure time of approximately 84 s. After this point the absorption effects are also observed to be negligible; i.e., we assume that $\alpha_0 = \alpha_1 = 0$.

Our fourth and final experiment involves examining the effects that mechanical vibrations have on the intensities of the two recording beams during saturation.

5. Effects of Mechanical Vibration

Much emphasis is placed on reducing mechanical vibration in holographic recording setups, for example, through the use of floating optical tables. The reason for trying to minimize these effects is that vibrations decrease the visibility of the recorded grating fringes owing to overwriting, producing smearing effects. The gratings recorded during this research were fabricated with a period of 1 μm. In this case a high-frequency relative in-plane motion of the plate during exposure of amplitude 0.5 μm could potentially eliminate the grating completely. We carried out a series of experiments, using plate holders with different levels of mechanical stability (rigidity). We note that the experimental results shown in Fig. 2 were produced by use of a relatively poor holder, which was not rigid. Therefore vibrational motion could occur. The mechanical shutter (Uniblitz shutter, controlled by a VMM-D1 shutter driver controller), used at the start of the exposure, has been found to be a significant potential source of mechanical noise in our setups. Such system noise can be minimized by use of a rubber damping material, i.e., Sorbothane,[20] which is a viscoelastic polymer. This material exhibits special viscoelastic properties of both liquids (viscous solutions) and solids (elastic materials). They combine shock absorption, vibration isolation, and vibration damping characteristics.

For the experimental results shown in Fig. 2 a large-intensity oscillation is observed during recording. We propose that, following a long period of exposure (by which time the grating is fully formed and absorption effects do not vary with time), the main cause of the intensity variations is in-plane mechanical vibrations.

We constructed a model describing the transmitted intensity from a lossless grating replayed simultaneously by the two recording beams by applying appropriate replay boundary conditions.[7] We then applied this model to determine the form of the relative in-plane motion of the grating from both of the simultaneously measured sets of intensity data corresponding to I_R and I_S.

To start, we measured the average intensity values of the two beams after saturation, shown in Fig. 2. The values found are $I_R = 0.56\,\mathrm{mW}$ and $I_S = 0.4\,\mathrm{mW}$. The field amplitudes used as part of the replay boundary conditions are thus given by $r = \sqrt{I_R}$ and $s = \sqrt{I_S}$. For an unslanted transmission grating the obliquity factors c_R and c_S are equal to $\cos\theta$, where θ is the incident angle of the exposing beams (Fig. 1). They are equal because of the symmetric illumination used when an unslanted grating was recorded. The boundary conditions must take account of the motion of the grating relative to the two beams. In-plane motion simply gives rise to a phase change between the two beams and the grating. It was assumed in the research reported in Ref. 7 that the reference wave, R, at the input boundary ($z = 0$) has unit amplitude $R(0) = 1$ and that as it propagates through the grating it couples to the diffracted wave, S. It was also assumed that $S(0) = 0$. Relative in-plane motion has no effect in this case. However, in our model the initial conditions used are

$$S(0) = s \times \exp[-iKdx(t)], \tag{10}$$

$$R(0) = r \times \exp[+iKdx(t)], \tag{11}$$

where $dx(t)$ is the relative in-plane movement of the plate.[21] The coupled-wave differential equations used to model this situation, in which n_1 is constant, the replay is on-Bragg, and we assume that losses are negligible, i.e., that $\alpha_1 = \alpha_0 = \kappa_i = 0$, are given by

$$cR'(z) + i\kappa_r S(z) = 0, \tag{12}$$

$$cS'(z) + i\kappa_r R(z) = 0, \tag{13}$$

z is the distance into the thickness of the material layer. These coupled equations are solved under the boundary conditions in Eqs. (10) and (11), and expressions for the transmitted intensities at $z = d$ are found:

$$I_R(t) = \frac{1}{2}\left\{r^2 + s^2 + (r^2 - s^2)\cos\left(\frac{2\kappa_r d}{c}\right) - 2rs\,\sin\left(\frac{2\kappa_r d}{c}\right)\sin[2Kdx(t)]\right\}, \tag{14}$$

$$I_S(t) = \frac{1}{2}\left\{r^2 + s^2 + (-r^2 - s^2)\cos\left(\frac{2\kappa_r d}{c}\right) - 2rs\,\sin\left(\frac{2\kappa_r d}{c}\right)\sin[2Kdx(t)]\right\}. \tag{15}$$

Given r, s, d, κ_r, c, K, and the Fresnel-corrected data for both I_R and I_S, estimates of the motion of the plate, $dx(t)$, can be obtained. A plot of the estimated motion of the plate extracted from Fig. 2 is shown in Fig. 6.

This motion, estimated from the measured data for both of the beams, I_R and I_S, should be equal for the two beams but does not coincide exactly because of (i) experimental errors, (ii) the simplicity of the coupled-wave model, and (iii) the simple form of in-plane motion assumed. However, good general agreement is found, which indicates that our in-plane motion assumption has some validity.

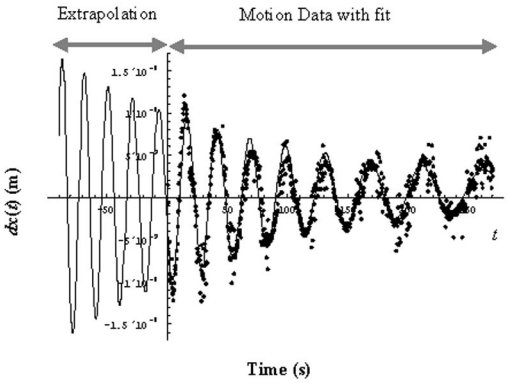

Fig. 6. Motion of the plate extracted from experimental data for both beams with a fit to the motion including extrapolation to estimate the motion before saturation.

Returning to the intensity data, we note that the frequency of the oscillations varies slightly as a function of time. Obtaining a best fit to the frequency variations of the oscillations, we should then be able to extrapolate our prediction for $dx(t)$ back into the growth region of the experimental data. We accomplish this by first converting the frequency variation in the saturation region into the corresponding phase variations. We then identify the points where the intensity data cross the intensity average as zero phase values. A piecewise linear representation of the phase variation is shown in Fig. 7. A cubic polynomial best fit to the phase of the form given in Eq. (16) below is used:

$$\phi(t) = a + bt + ct^2 + dt^3. \tag{16}$$

Typical coefficients obtained for the best-fit polynomial were $a = 0.284$, $b = 0.274$, $c = 0.0004$, and $d = 2.28 \times 10^{-7}$. Then, using this expression for the phase, we proceed, using the analytic function shown

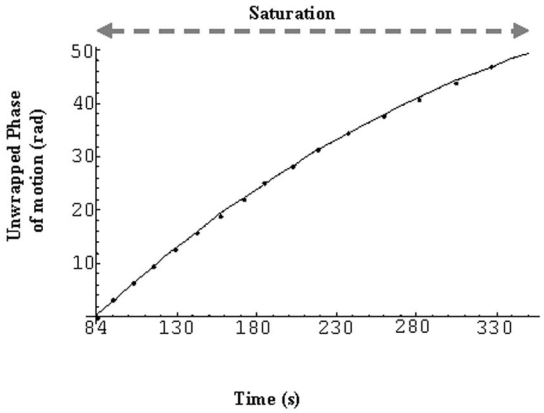

Fig. 7. Phase variations with time for the R beam (unwrapped). A similar plot was obtained for the S beam.

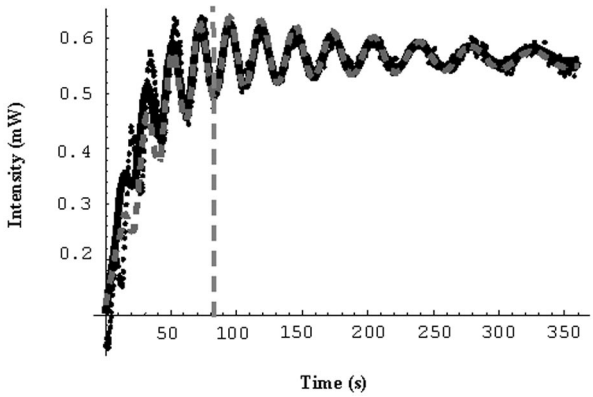

Fig. 8. Experimental data for the intensity of the R beam (filled circles), theoretically fitted to the data with $\kappa_i = 0$ (thin dashed line), and including the lossy grating, where $\kappa_i \neq 0$ (thick dashed curve).

in the following equation, to find a least-squares fit to describe the in-plane motion of the plate:

$$dx(t) = A + B\,\exp(-Ct)\sin[\phi(t)]. \tag{17}$$

The exponential is introduced into the fitting function because the amplitude of the oscillation in Fig. 6 is observed to decrease with time. Typical values of $A = 1 \times 10^{-8}$, $B = -2 \times 10^{-8.3}$, and $C = -0.0065$ were found.

Having defined Eq. (17), we can make predictions about the motion during the growth of the phase grating, i.e., during the first 84 s of the recorded data. Back interpolation provides a crude approximation to the motion of the plate from the moment the shutter opens until saturation is reached. Figure 6 shows the predictions of the analytic best fit to the motion in both regions. Combining this result and the three previous experimental results, we can now provide a fit to the complete experimental data set originally presented in Fig. 2.

6. Combined Model

We wish to fit the data presented in Fig. 2 that describe the modulation of the transmitted beams. From these data we were able to analyze the different processes involved in recording a holographic grating. From the second experiment we were able to express the absorption of the material, $\alpha_0(t)$, as a function of time. The third experiment enabled us to obtain an expression for lossless grating strength $\nu(t)$, as the grating was being grown. From the fourth experiment we derived an expression for the motion of the plate relative to the exposing beams as a function of time, d$x(t)$. All these expressions are now substituted into the two first-order coupled-wave equations, which are thus modified to allow for the time evolution of all the major (decoupled) grating parameters during exposure:

$$cR'(z) + i[\kappa_r(t) + i\kappa_i(t)]S(z) + \alpha_0(t)R(z) = 0, \tag{18}$$

$$cS'(z) + i[\kappa_r(t) + i\kappa_i(t)]R(z) + \alpha_0(t)S(z) = 0. \tag{19}$$

In particular, we note that, although we have no analytic expression for $\alpha_1(t)$, the effects of the time-varying lossy grating amplitude is retained in this analysis. We solve Eqs. (18) and (19), using the boundary conditions presented in Eqs. (10) and (11) at $z = d$, obtaining

$$\begin{aligned} I_R(t) = \frac{1}{4}\exp\left\{-\frac{2d[\alpha_0(t) + \kappa_i(t)]}{c}\right\} \\ \times \left(\left\{1 + \exp\left[\frac{4d\kappa_i(t)}{c}\right]\right\}(r^2 + s^2)\right. \\ + 2\left\{-1 + \exp\left[\frac{4d\kappa_i(t)}{c}\right]\right\}\{rs\,\cos[2Kdx(t)]\} \\ + 2\exp\left[\frac{2d\kappa_i(t)}{c}\right]\left\{(r-s)(r+s)\cos\left[\frac{2d\kappa_r(t)}{c}\right]\right\} \\ \left. - 2rs\,\sin[2Kdx(t)]\sin\left[\frac{2d\kappa_r(t)}{c}\right]\right), \end{aligned} \tag{20}$$

$$\begin{aligned} I_S(t) = \frac{1}{4}\exp\left\{-\frac{2d[\alpha_0(t) + \kappa_i(t)]}{c}\right\} \\ \times \left(\left\{1 + \exp\left[\frac{4d\kappa_i(t)}{c}\right]\right\}(r^2 + s^2)\right. \\ + 2\left\{-1 + \exp\left[\frac{4d\kappa_i(t)}{c}\right]\right\}\{rs\,\cos[2Kdx(t)]\} \\ - 2\exp\left[\frac{2d\kappa_i(t)}{c}\right]\left\{(r-s)(r+s)\cos\left[\frac{2d\kappa_r(t)}{c}\right]\right\} \\ \left. - 2rs\,\sin[2Kdx(t)]\sin\left[\frac{2d\kappa_r(t)}{c}\right]\right). \end{aligned} \tag{21}$$

Equations (20) and (21) are then used to fit the full data curves with the hope of accurately describing the modulation of the recording beams' data during grating formation and saturation. Plots of $I_R(t)$ [Eq. (20)] and the corresponding experimental data, assuming that κ_i is negligible, are shown in Fig. 8.

Also, a plot of Eq. (20) including κ_i is shown in Fig. 8, where $\alpha_1(t)$ has the form that was presented in Eq. (6) and Fig. 5. The form chosen met certain conditions: all time-varying absorption effects happened within the first 84 s [therefore, when $t = 84$ s, $\alpha_1(t) \cong 0$] and the size of $\alpha_1(t)$ at all times was less than $\alpha_0(t)$. These conditions place constraints only on the possible form of the behavior of the lossy grating. The values for the coefficients in Eq. (6) that govern the form chosen are $p = 0.05$ and $q = 0.08$.

An accurate model for its behavior must be found to improve the overall fit to the experimental data. But, as can be seen from Fig. 8, the inclusion of the values used for the lossy grating in the analysis (even though it is not an accurate model of its behavior) can be used to improve the fit to the experimental data. Similarly acceptable fits can also be found to the $I_S(t)$ data.

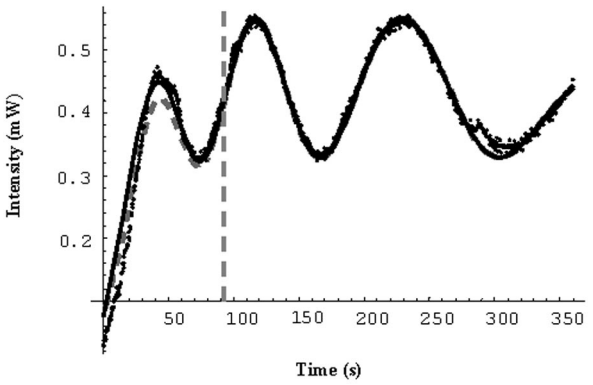

Fig. 9. S beam intensity data, with an almost unity beam ratio (filled circles), with a theoretical fit to the data where $\kappa_i = 0$ (dashed line) and a fit to the data including the lossy grating, i.e., where $\kappa_i \neq 0$ (solid curve).

The above analysis was repeated several times for data sets produced with beam ratios closer to unity. For the experimental data shown in Fig. 9, the R beam intensity is $I_R = 0.45$ mW and the S beam intensity is $I_S = 0.42$ mW. The resultant theoretical fit to those data, where κ_i was assumed to be negligible for the S beam is shown in Fig. 9. An improved fit could be achieved when the lossy grating was included in the analysis, as shown by the solid curve in Fig. 9. A form for the lossy grating similar to that used for Fig. 8 was used, with the coefficients in Eq. (6) given by $p = 0.05$ and $q = 0.03$.

7. Conclusions

In this paper one possible explanation for the modulation of the recording beams that is sometimes observed when sinusoidal unslanted gratings are recorded has been proposed. A first-order analysis was presented, which assumes that different parts of the physical recording process can be decoupled. The simple phenomenological model proposed incorporates the growth of the phase grating, time-varying absorption effects, in-plane motion of the plate owing to vibration, growth of a lossy absorption grating during recording, and the effects of beam ratio to explain the beam modulation.

A series of experiments was carried out to provide an empirical basis for our model. The first experiment involved measuring the transmitted intensities of the two exposing beams to permit us to examine their variation as a function of time. As modulation in the beams does not always occur, this experiment was rerun a number of times with different plate holders of different rigidity. Several beam ratios were also used when we examined the modulation effects. Two particular sets of data were presented here for different beam ratios; the resultant intensity oscillations differed significantly. In both cases the intensity oscillations measured are in agreement with the predictions of our model and as predicted become more significant for nonunity recording beam ratios.

The second set of experiments examined the effect the absorption of the material has on a single beam as a function of time.[22,23] The same standard layer thickness and composition were used in all the experiments discussed, and an empirical expression for the absorption coefficient was presented.

The third set of experiments examined the growth of the lossless phase grating. By capturing the growth curves of gratings, using a probe beam of a different wavelength that is unaffected by the dye, we found the grating's refractive-index modulation and in particular the maximum or saturation value.

The fourth and final experimental results presented involve the determination of the motion of the grating with respect to the two exposing beams. The magnitude of this motion was found to decrease from maximum amplitudes of approximately 30 nm in the case of Fig. 8 and of approximately 20 nm in the case of Fig. 9. We note that the amplitude and frequency of the oscillations varied among setups, indicating some dependence on the recording setup. As mentioned, one plausible source of the vibrations is the Uniblitz mechanical shutter, and damping the shutter, increasing the rigidity of the plate holder, or both was found to reduce these effects.

We note that the motion present is large enough to cause some smearing of the grating during recording. We also expected some variation of the exposing beam's pattern amplitude with depth. All such effects are completely neglected in our analysis.

When one is recording, it is desirable to have unity beam ratio, because this produces maximum fringe visibility. We note that both our model and data indicate that if the beams are unequal, the effects of modulation in intensity are more significant.

To increase the validity of our model we included the effects of the formation of an absorption grating that arise as results of the dye. As shown in Fig. 9, the inclusion of a physically reasonable lossy grating can improve the fit to the experimental data. However, the form and size of the lossy grating must be further studied.[9] Changes in the exposing intensity as a function of both time and depth within the material are important. Recently attempts to predict three-dimensional behavior in photopolymers were reported.[10] Inclusion of these effects and also the variation of average intensity I_0 within the material with any time variation of the absorbance of the dye[24] are currently being investigated.

It is assumed that only in-plane motion of the plate occurs; the other five degrees of freedom available are neglected. However, as noted, assuming simple motion, the vibrations estimated by use of the R and S beams are not exactly equal. Therefore other types of motion are taking place and should be included in the model. Furthermore, as the largest amplitude of motion occurs at the start of the exposure, it is possible that nonlinear mechanical coupling takes place at that time.

Experiments are currently being carried out to measure the vibrations present in our system on the interference pattern produced by the two plane waves used for recording. The movement of the fringes can be observed and qualitatively matches the behavior

estimated. Quantitative correlation remains to be achieved.

Any significant improvements to our approximate model will necessitate including rigorous electromagnetic analysis, including time variation effects, with the material models describing the grating formation process. An example of one such material model is the nonlocal polymer driven diffusion model.[25,26]

We conclude by noting that, despite all the assumptions made, our first-order phenomenological model is plausible and physically appealing and provides insights into and general agreement with the experimental data measured.

The authors acknowledge the support of Enterprise Ireland and Science Foundation Ireland through the Research Innovation Fund and the Basic Research Program. F. T. O'Neill currently holds an Embark (Irish Research Council for Science, Engineering and Technology) postdoctoral research fellowship.

References

1. F. T. O'Neill, J. R. Lawrence, and J. T. Sheridan, "Automised testing and recording of holographic optical element arrays," Optik (Stuttgart) **111,** 459–467 (2000).
2. M. R. Gleeson, F. T. O'Neill, and J. T. Sheridan, "Modulation of recording beams during grating formation," in *Photon Management*, F. Wyrowski, ed., Proc. SPIE **5456,** 285–296 (2004).
3. M. R. Gleeson, F. T. O'Neill, and J. T. Sheridan, "Recording beam modulation during grating formation," in *Organic Holographic Materials and Applications II*, K. Meerholtz, ed., Proc. SPIE **5521,** 149–160 (2004).
4. W. L. Wilson, InPhase Technologies (www.inphase-tech.com; personal communications, 2003).
5. J. R. Lawrence, F. T. O'Neill, and J. T. Sheridan, "Photopolymer holographic recording material," Optik (Stuttgart) **112,** 449–463 (2001).
6. LabView User's Manual (National Instruments Corporation, Austin, Tex., January 1998), pp. 2–12.
7. H. Kogelnik, "Coupled wave theory for thick holographic gratings," Bell Syst. Tech. J. **48,** 2909–2947 (1969).
8. S. Caron, J. J. A. Couture, and R. A. Lessard, "Real time holographic reinforcement demonstrated by thionine/PVA photoreducible thin layers," Appl. Opt. **29,** 599–603 (1990).
9. S. Caron, R. A. Lessard, and P. C. Roberge, "Photodarkening and partial photobleaching: application to dichromated gelatin," Appl. Opt. **40,** 707–713 (2001).
10. S. Gallego, M. Ortuño, C. Neipp, A. Márquez, A. Beléndez, I. Pascual, J. V. Kelly, and J. T. Sheridan, "Physical and effective optical thickness of holographic diffraction gratings recorded in photopolymers," Opt. Express **13,** 1939–1947 (2005).
11. A. V. Galstyan, R. S. Hakobyan, S. Harbour, and T. Galstian, "Study of the inhibition period prior to the holographic grating formation in liquid crystal photopolymerizable materials," Electronic-Liq. Cryst. Commun. (www.e-lc.org/docs/2004_05_05_11_13_17/).
12. Y. L. Lee, C. H. Kwak, J. H. Kwon, Y. S. Im, and O. S. Choe, "Observation of a fast formed absorbtion grating and a slowly formed phase grating in undeveloped dichromated gelatin," Appl. Opt. **40,** 3635–3639 (2001).
13. J. V. Kelly, M. R. Gleeson, C. E. Close, F. T. O'Neill, J. T. Sheridan, S. Gallego, and C. Neipp, "Temporal and non-ideal behaviour in photopolymers," in *Opto-Ireland 2005: Photonic Engineering*, B. W. Bowe, G. Byrne, A. J. Flanigan, T. J. Glynn, J. Magee, G. M. O'Connor, R. O'Dowd, G. D. O'Sullivan, and J. T. Sheridan, eds., Proc. SPIE **5827,** 95–106 (2005).
14. C. Carre and D. J. Lougnot, "Photopolymerizable material for holographic recording in the 450–550 nm domain," J. Opt. (Paris) **21,** 147–152 (1990).
15. F. T. O'Neill, J. R. Lawrence, and J. T. Sheridan, "Improvement of holographic recording material using aerosol sealant," J. Opt. A Pure Appl. Opt. **3,** 20–25 (2001).
16. F. T. O'Neill, J. R. Lawrence, and J. T. Sheridan, "Thickness variation of self-processing acrylamide based photopolymer and reflection holography," Opt. Eng. **40,** 533–539 (2001).
17. R. R. A. Syms, *Practical Volume Holography* (Clarendon, 1990).
18. E. Hecht, *Optics*, 2nd ed. (Addison-Wesley, 1987).
19. M. Born and E. Wolf, *Principles of Optics*, 6th ed. (Pergamon, 1980).
20. www.edmundoptics.com.
21. J. T. Sheridan, "Stacked volume holographic gratings: Part I, Transmission gratings in series," Optik (Stuttgart) **95,** 73–80 (1993).
22. N. Capolla and R. A. Lessard, "Processing of holograms recorded in Methylene Blue sensitized gelatin," Appl. Opt. **27,** 3008–3012 (1998).
23. C. Solano, R. A. Lessard, and P. C. Roberge, "Methylene Blue sensitized gelatin as a photosensitive medium for conventional and polarizing holography," Appl. Opt. **26,** 1989 (1987).
24. S. Blaya, L. Carretero, R. F. Madrigal, M. Ulibarrena, P. Acebal, and A. Fimia, "Photopolymerization model for holographic gratings formation in photopolymers," Appl. Phys. B **77,** 639–662 (2003).
25. J. T. Sheridan and J. R. Lawrence, "Non-local response diffusion model of holographic recording in photopolymer," J. Opt. Soc. Am. A **17,** 1108–1114 (2000).
26. J. V. Kelly, F. T. O'Neill, J. T. Sheridan, C. Neipp, S. Gallego, and M. Ortuno, "Holographic photopolymer materials: nonlocal polymerization driven diffusion under nonideal kinetic conditions," J. Opt. Soc. B **22,** 407–416 (2005).